Faraday Discussions

Accepted Manuscript

This manuscript will be presented and discussed at a forthcoming Faraday Discussion meeting. All delegates can contribute to the discussion which will be included in the final volume.

Register now to attend! Full details of all upcoming meetings: http://rsc.li/fd-upcoming-meetings

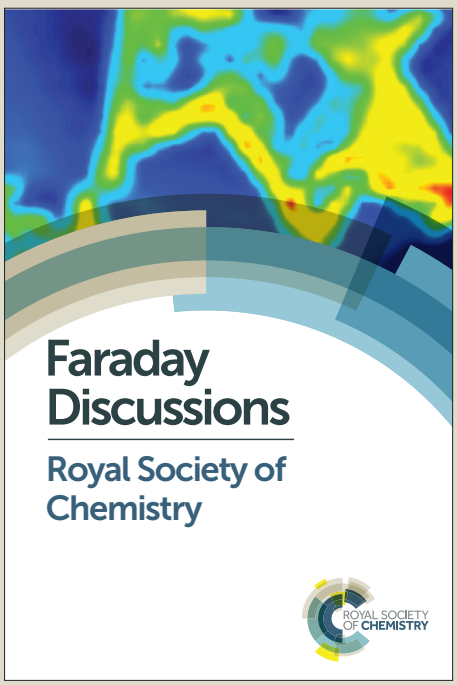

This is an *Accepted Manuscript*, which has been through the Royal Society of Chemistry peer review process and has been accepted for publication.

Accepted Manuscripts are published online shortly after acceptance, before technical editing, formatting and proof reading. Using this free service, authors can make their results available to the community, in citable form, before we publish the edited article. We will replace this *Accepted Manuscript* with the edited and formatted *Advance Article* as soon as it is available.

You can find more information about *Accepted Manuscripts* in the Information for Authors.

Please note that technical editing may introduce minor changes to the text and/or graphics, which may alter content. The journal's standard Terms & Conditions and the Ethical guidelines still apply. In no event shall the Royal Society of Chemistry be held responsible for any errors or omissions in this *Accepted Manuscript* or any consequences arising from the use of any information it contains.

ROYAL SOCIETY OF CHEMISTRY

www.rsc.org/faraday_d

Faraday Discussions

RSCPublishing

ARTICLE

Design of FeBi nanoparticles for imaging applications

Cite this: DOI: 10.1039/x0xx00000x

M. Branca,[a,b] F. Pelletier,[a,b], B. Cottin,[a,b] D. Ciuculescu,[a,b] C.-C. Lin,[c] R. Serra,[d,b] J.-G. Mattei,[d,b] M.-J. Casanove,[d,b] R. Tan,[e,b] M. Respaud[e,b] and C. Amiens*[a,b]

Received 00th January 2012,
Accepted 00th January 2012

DOI: 10.1039/x0xx00000x

www.rsc.org/

A variety of imaging technologies are now routinely used in the medical field, their use being continuously enlarged through the development of contrast agents. Recently nanoparticles (NPs) proved efficient to improve imaging *in vivo* by increasing contrast and targeting capabilities. The current trend is now focused on the development of dual contrast agents combining two or more functionalities on the same NP. Motivated by this new challenge we developed FeBi NPs as new nanomaterials with potential application as contrast agent for MRI and CT imaging. In addition to the well-known use of iron in the development MRI contrast agents, we chose Bi as CT imaging agent rather than the more documented gold, because it possesses a larger X-ray attenuation coefficient and is much less expensive. Two sets of NPs, with sizes around 150nm and 14nm, were synthesized using organometallic approaches. In both cases, NPs are spherical, and contain distinct domains of Fe and Bi, the surface being enriched in Fe, and a hydrophobic coating. This coating differs from one sample to the other: the surface of the 150nm large NPs is coated by amine ligands, while that of 14nm large NPs is coated by a mixture of an amine and its hydrochloride salt. Exchange of the surface ligands to afford water soluble NPs has been attempted. We show that only the larger NPs could be functionalized with water soluble ligands, in agreement with the lability of their initial surface coating. Colloidal aqueous solutions of FeBi NPs with glycoPEG ligands have been obtained.

Introduction

Today's capabilities in clinical diagnostic radiology have been made possible by advances not only in diagnostic systems, but also by the contrast media and radiopharmaceuticals that make it possible to see, in great detail, the body's internal structures, organs and tissues that would not otherwise be clearly seen. Among these, nanoparticles (NPs) play an increasing role as their larger size compared to molecular contrast agents increases their residence time in the body. [1] Superparamagnetic Iron Oxide Nanoparticles (SPION) are already commercially available as contrast agents for magnetic resonance imaging (MRI), fluorescent nanoparticles (quantum dots) are also well-known for optical detection and nanohybrids are developed to replace the currently used iodine-based contrast agents in Computed X-Ray Tomography (CT), among which bismuth derivatives are reported as very promising.[2,3,4,5] The use of NPs also facilitates the functionalization, and thus targeting, of the contrast agent.[6,7,8,9] As no single imaging modality can address all biological questions, the next step to further improve diagnostics lies in the development of dual contrast agents (coupling of T1/T2 MRI contrast agents,[10,11] optical and radioemitting probes,[12] MRI and fluorescent markers[13] or other optical probes,[14] ultrasonography and MRI,[15,16] MRI and CT[17]…), which will give better resolved images and rule out artifacts, hence help define the most appropriate treatment.[18] Especially, a dual CT/MRI contrast agent would help improve the diagnostics of cardiovascular diseases,[19] or the optimization and follow-up of embolization therapies.[20]

Faraday Discussions Accepted Manuscript

In this context, associating iron oxide and bismuth inside a nano-object looks promising as 1) SPION are already in use as MRI contrast agents, 2) bismuth NPs have been demonstrated to give good contrast in CT[2-4,21] with low toxicity reported so far, and 3) both materials are of low cost. It is noteworthy that a nanohybrid associating Fe and Bi was published recently by Andres-Verges et al.[22] In this work each NP consists in an iron oxide core and a bismuth oxide shell. However, optimum arrangement of the Fe and Bi domains in the nanohybrids should comprise a bismuth core (to minimize bismuth interaction with the biological material to be imaged) and an iron shell, thus insulating the bismuth component and maximizing the interaction between the magnetic component and the water protons which is important to reach a good contrast in MRI as shown by Kim et al.[17]

We herein report on the organometallic synthesis of BiFe NPs with a surface enriched in Fe. Depending on the synthetic process, NPs of different average size (150 or 14nm) and surface chemistry (amine or a mixture of amine and its hydrochloride salt) could be obtained. We show that the initial surface coating is a key-parameter for the further functionalization of the NPs and their transfer into water, the first requisite before any use of these NPs as contrast agents for biomedical imaging. Preliminary results on the X-ray opacity and possible use of these nanohybrids as MRI contrast agents are also reported for the NPs with the optimum size.

Experimental

Materials and methods

All the syntheses were performed under argon atmosphere by using Fischer–Porter bottles techniques, glove box and argon/vacuum lines. $[Fe(N(SiMe_3)_2)_2]$ (>99%) was purchased from Nanomeps, HDA(99%), and anhydrous anisole from Sigma-Aldrich. Anisole was further purified by distillation under argon (over sodium), degassed by the freeze-pump-thaw technique and dried over molecular sieve (0.4nm) before use.

$Bi(N(SiMe_3)_2)_3$,[23] HDA.HCl[24] and $iPr_2NH{-}BH_3$[25] were prepared and purified according to published procedures.

Dihydrogen was purchased from Air Liquide. It contained less than 3 ppm of H_2O and 2 ppm of O_2. To determine the Fe and Bi contents in the materials, elemental analyses were performed at Antellis[26] by ICP-MS (Inductively Coupled Plasma-Mass Spectrometer), after digestion of the samples in concentrated HNO_3.

Synthetic procedures

- **Synthesis of 150nm large BiFe NPs (sample BiFe150)**

$Fe(N(SiMe_3)_2)_2$(80 mg, 0.21 mmol), $Bi(N(SiMe_3)_2)_3$ (20mg, 0.03 mmol), HMDS (343 mg, 2.1 mmol) were dissolved in anisole (18 mL, H_2O < 3ppm) in a Fischer-Porter bottle in a glove box. The homogeneous yellow-green solution was freezed under liquid nitrogen and 1.1 equivalent of diisopropylamine-borane with respect to iron (27 mg, 0.24 mmol) in anisole (4 mL) were canula-transferred in the Fischer-Porter bottle. Slow warm-up of the reaction medium up to room temperature afforded a dark brown solution. This homogeneous solution was then pressurized with 3 bar H_2 and heated 4h at 110°C, and 19h at 150°C without any stirring. A black magnetic solid was recovered by filtration, washed with anisole (5 mL) and dried under vacuum. (recovered mass: 16mg; Fe: 11.18% ; Bi: 5.52 % i.e. atomic composition Fe7.6Bi1).

- **Synthesis of 14nm large BiFe NPs (sample BiFe14)**

In a typical synthesis the reaction mixture is prepared in a glove box as follows: in a Fischer-Porter bottle, $Fe[N(Si(CH_3)_3)_2]_2$ (376 mg, 1 mmol) and $Bi[N(Si(CH_3)_3)_2]_3$ (68.9 mg, 0.1 mmol) are dissolved in 20mL of dry anisole. HDA (483 mg, 2 mmol) and HDA.HCl (415 mg, 1.5 mmol) are subsequently added. The color of the solution turns progressively from green-yellow to brown. After this, the reactor is immersed in an oil bath preheated at 150°C and kept at this temperature under magnetic stirring for 5 hours. The reaction is then allowed to return to room temperature and the solvent is removed by evaporation under reduced pressure. The residue is washed with 40 mL of toluene. (recovered mass: 200mg. 15%Fe, 4%Bi)

- **Control experiment**

$Bi[N(Si(CH_3)_3)_2]_3$ (68.9 mg, 0.1 mmol) is dissolved in 20mL of dry anisole. HDA (483 mg, 2 mmol) is subsequently added. After this, the reactor is immersed in an oil bath preheated at 150°C and kept at this temperature under magnetic stirring. The color of the solution turns progressively from yellow to brown and black over a 1/2hour. Heating is continued for 5hours, then the reaction is allowed to return to room temperature and the solvent is removed by evaporation under reduced pressure. The solid recovered (mass: 176mg) was directly analysed by FT-IR spectroscopy.

- **Synthesis of modified PEG ligands**

LPEG1 and LPEG2 have been prepared according to already published procedures.[27]

- **Water transfer**

The NPs (3mg) and the selected PEG ligand (5mg) are suspended in a 1/1 (v/v) water /methanol mixture. After sonication for 20mn, a homogeneous black solution is obtained. The modified NPs are recovered by centrifugation and redispersed in water. Then, two other centrifugation steps are carried out to remove excess PEG ligand. The final powder is dried under vacuum (5mg). It can be easily redispersed in water but the NPs settle after 6 (LPEG1) to 20mn (LPEG2).

Characterization techniques

- **FT-IR:**

FTIR spectra of Bi nanoparticles, in powder form, were recorded in the glove box on a Bruker ALPHA spectrometer in ATR mode on a diamond crystal.

- **TEM and EDS experiments:**

The nano-objects were deposited on carbon-coated copper grids by casting a drop of a THF or anisole solution of the nanoparticles powders.

Conventional TEM and HREM images were obtained on JEOL microscopes respectively JEM1011 (100kV), and JEM2100F (200kV) with a spatial resolution of 0.23nm at the TEMSCAN facility at Université Paul-Sabatier. EDS spectra were recorded in STEM mode on the JEOL JEM 2100F TEM-FEG (at

Faraday Discussions Accepted Manuscript

 This journal is © The Royal Society of Chemistry 2012

TEMSCAN, UPS) or CEM20 FEI (at CEMES) microscopes fitted with a Bruker QUANTAX EDS system.
HREM experiments were carried out at CEMES, on a Cs-corrected FEI TECNAI F20 microscope, with point resolution of 0.12 nm and energy resolution of 0.8eV. The specimens were analyzed in this microscope before oxidation thanks to the use of a dedicated specimen holder fitted with an environmental cell, and after 2 days of air exposure. HREM images were acquired and processed using the Gatan Digital Micrograph environment.

- **Titration of galactose**

UV-visible spectra were recorded on a Perkin Elmer Lambda 35 spectrophotometer from 2mL of the solutions placed in 1cm thick glass cuvets. Galactose, was determined by the anthrone/sulfuric acid method. Briefly, 0.5mL of D-galactose standard solutions (0, 40, 60, 80, 100, 120 $\mu g.mL^{-1}$), or 0.5mL of NPs solutions (50mg/mL) are introduced in a test tube in the presence of 1mL of anthrone reactant (60mg of anthrone in 30mL of concentrated sulfuric acid) and heated at 85°C for 10mn. 0.5 mL of the green solutions obtained are then diluted with 2mL of concentrated sulfuric acid. The absorbance of each of the standards and samples was measured (626 nm) and the galactose content of the NPs was interpolated from a standard curve prepared in this manner.

The coverage of galactose at the surface of the NPs was thus derived knowing the % of surface atoms in the NPs dispersion (3.4% per NP given their size and morphology). LPEG1 : 20% ; LPEG2 : <10%.

Results and discussion

Synthesis and structural characterisation

From a thermodynamic point of view, as Fe and Bi are immiscible, Bi having the lowest surface tension and the largest atomic radius should segregate at the surface of the NP. To circumvent this problem we have relied on kinetically controlled growth processes. We have already demonstrated in the case of FeRh system that controlling the kinetics of production of each element allowed a precise control over the chemical order inside the NP from a Rh core/Fe shell structure to the reverse situation, namely Fe core and Rh rich shell.[28,29] It is noteworthy that this second arrangement corresponds to a metastable chemical distribution. We thus decided to follow this strategy to build Bi@Fe core-shell NPs. Based on previous results, we have designed two different pathways starting in each case from a homogeneous solution of the Bi and Fe homoleptic amido complexes: $[Bi((N(SiMe_3)_2)_3]$ and $[Fe((N(SiMe_3)_2)_2]$.
In a first process (P1) we use amine-borane as a reducing agent to produce Fe atoms from $[Fe((N(SiMe_3)_2)_2]$. These atoms are thus generated in the presence of the oxidizing $[Bi((N(SiMe_3)_2)_3]$ complex. A fast galvanic displacement follows regenerating the Fe precursor and producing Bi atoms which evolve into Bi NPs, the core of the expected Bi@Fe NPs. Following this first step, pressurization of the reacting medium under 3bar H_2 ensures reduction of the Fe precursor and deposition of Fe atoms on top of the first formed Bi seeds.

Analysis of the sample has evidenced NPs of average diameter 150nm with a bismuth enriched core and iron rich surface (Figure 1), as the result of the very precise design of the kinetics of reaction of each metal complex, where iron acts as a catalyst for the reduction of the poorly reactive bismuth precursor.[30] The sample obtained is called BiFe150 in the following.

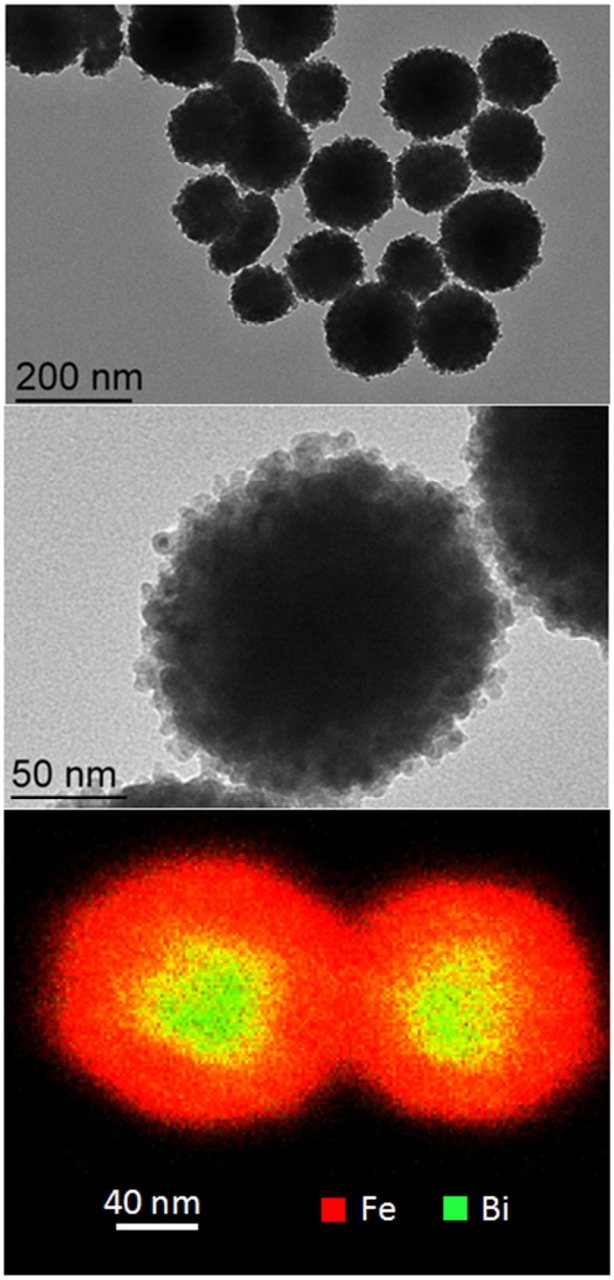

Figure 1: top and middle: typical TEM images of NPs from BiFe150; bottom: EDS analysis showing the chemical distribution in the NPs.

A second possibility to kinetically differentiate the reduction of these Fe and Bi precursors relies on the use of long chain amine as reducing agents. To investigate this possibility we chose hexadecylamine which is frequently used as both reducing and

Faraday Discussions Accepted Manuscript

stabilizing agent in nanochemistry. A control experiment followed by FT-IR spectroscopy shows that the Bi precursor starts decomposing at room temperature and is fully decomposed after 5h of reaction at 150°C (not shown). On the other hand, literature reports that the Fe precursor requires a temperature above 110°C to be reduced,[31] and is only fully decomposed after 48h at 150°C. This confirms the possibility to control the chemical order of the final BiFe NPs based on kinetics of reactions.

TEM analysis of this material (Figure 2) evidences an average size of 14 nm, with a standard deviation of 4 nm according to a Gaussian fit of the size distribution. Accordingly the sample will be called BiFe14 hereafter. A light shell and a dark crystalline core are observed suggesting a core-shell distribution of the two elements with bismuth the heaviest located in the core of the NPs. However, a more careful analysis is needed to ascertain this point, as this contrast is also the expected contrast for a spherical object, the thicker region of the core being much more absorbent for the incident electron beam than the surface region. EDS analysis has been carried out on individual NPs. As can be observed in Figure 2 (bottom), the signal over noise ratio is low due to the small size of the objects under study (although EDS analysis was carried out on the largest nanoparticles found in the preparation). Still, it also suggests the presence of Bi in the core of the NPs while the surface seems to be mainly constituted of iron. Analysis of HREM images further allows determining the nature and structure of the nanodomains. For this purpose, HREM images were recorded using a dedicated TEM specimen holder fitted with an environmental cell in order to protect the specimen from oxidation during transfer from the glove box to the microscope. Investigation of the outer iron layer of the NPs evidences the presence of densely packed iron nanograins some of them adopting a *bcc* structure. e.g. on Figure 3, a small bcc iron grain is observed along the [111] zone axis in the left side of the particle. In the core of the NPs, lattice planes can be observed, the spacing of which (0.328 nm) is in agreement with the formation of a single crystalline bismuth domain of *rhombohedral* structure.

The observed chemical order is thus in complete agreement with the relative kinetics of reduction of the two metal precursors which should generate Bi atoms in the reacting medium first, and Fe ones later on. From the average thickness of the iron shell (around 1.5 nm) and average size of the bismuth core (around 11 nm) one can estimate the atomic composition of the Bi@Fe nanoparticles to be around $Bi_{20}Fe_{80}$.

Water transfer.

As produced BiFe NPs are hydrophobic and soluble only in organic solvents such as THF, anisole, or toluene… It is noteworthy that the most reliable and versatile routes to obtain large quantities of NPs of good size, shape, crystallinity, and surface control, are developed in organic solvents and afford hydrophobic NPs. Therefore many methodologies have been developed to transfer them into water when required by the application (e.g. use in green catalysis or in the biomedical field). Among these, three main paths arise: ligand exchange, coating with amphiphilic ligands or polymers, or coating with a water soluble oxide shell such as silica. These main paths are depicted in Figure 4.

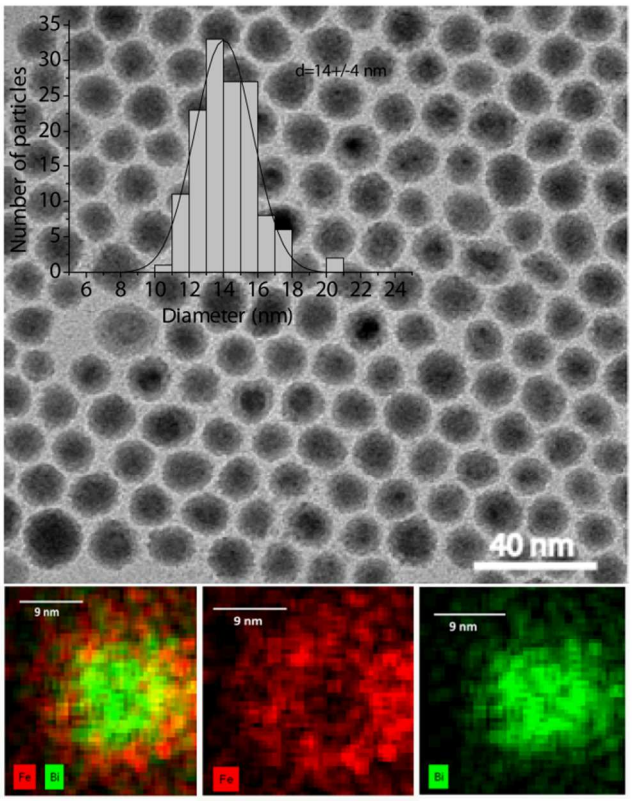

Figure 2: TEM image with size histogram of NPs from BiFe14 (top) and EDS analysis on an isolated NP (bottom)

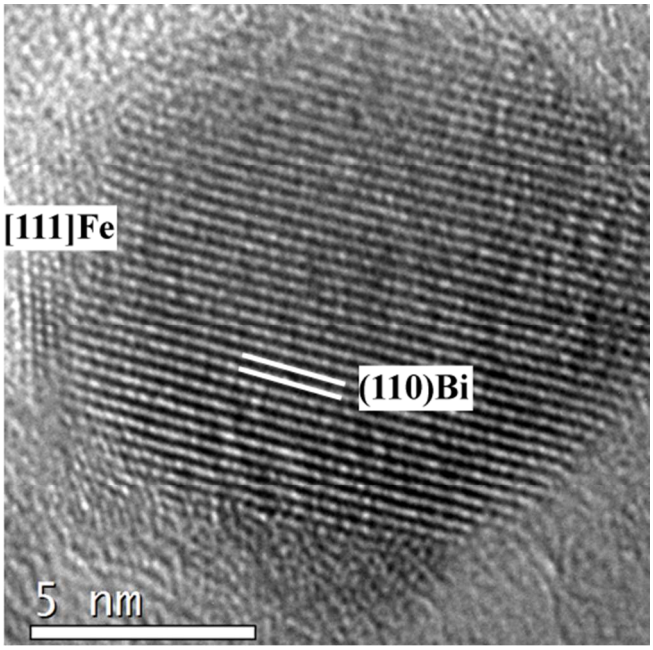

Figure 3: HREM image of an isolated NP from BiFe14

Faraday Discussions Accepted Manuscript

This journal is © The Royal Society of Chemistry 2012

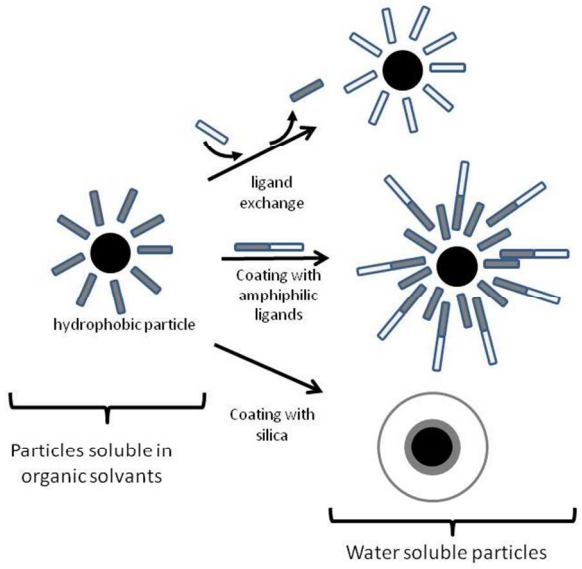

Figure 4: Main approaches to transfer hydrophobic NPs into water.

As ligand exchange at the surface of Fe NPs is well-known, we attempted this approach to change the hydrophilic balance of the BiFe NPs. Anticipating surface oxidation upon water transfer, we resorted to ligands capable of a strong binding both on iron and iron oxide surfaces such as carboxylic acid moieties.[32] The chosen ligands, hereafter called LPEG1 and LPEG2 are depicted in Figure 5. They are composed of a PEG chain and a galactose unit to provide water solubility, biocompatibility and futur targeting towards hepatocytes and hepatomas. Indeed, it is reported that galactose-derivatized superparamagnetic iron oxide NPs can be targeted specifically to hepatocytes and hepatomas due to the presence of asialoglycoprotein receptors on their cell surface.[33] Targeting of BiFe NPs would allow an accurate monitoring of liver cancers by coupling CT and MRI measurements. Furthermore these ligands bear a pendant carboxylic acid function to attach onto iron and iron oxide surfaces.

Incubation of BiFe150 NPs with the galactose ligands lead to its anchoring at the surface of the NPs, as schematically represented in Figure 6 (top). Water transfer could be achieved. This further attests the high lability of amine, and especially HMDS, at the NPs surface.

Stability of the colloidal solution varies as a function of the ligand used. As expected, longer PEG chains ensure better solubility.

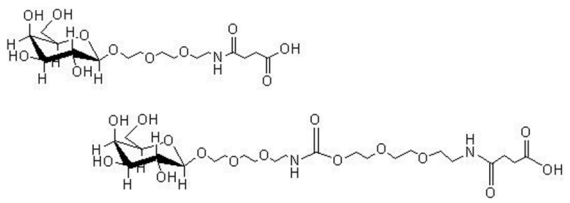

Figure 5: structure of LPEG1(top) and LPEG2 (bottom)

UV-vis estimation of galactose content was carried out following the Dreywood's analytical method.[34] Surface coverage was found to be around 20% for LPEG1 and below 10% for LPEG2. The lower surface coverage for LPEG2 can be explained by the ability of PEG chains to coil upon themselves.[35,36] However, this generally occurs for much longer polymer chains and suggests that the galactose moiety has a role to play in the conformation of the ligand at the surface of the NPs. Especially one cannot discard the possibility of interactions between the -OH groups of galactose and the Fe surface atoms. This phenomenon can occur already for LPEG1 as the surface coverage is quite low compared to that reported for e.g. mercapto-PEG ligands of comparable length and could explain the limited stability of the aqueous solutions obtained.[37] Still, despite a lower coverage, NPs stabilized with LPEG2 display a better solubility in water than those stabilized by LPEG1. Interestingly the NPs still responded to an applied magnetic field. This observation is important in view of the application as MRI contrast agent as this technique relies on the magnetization.

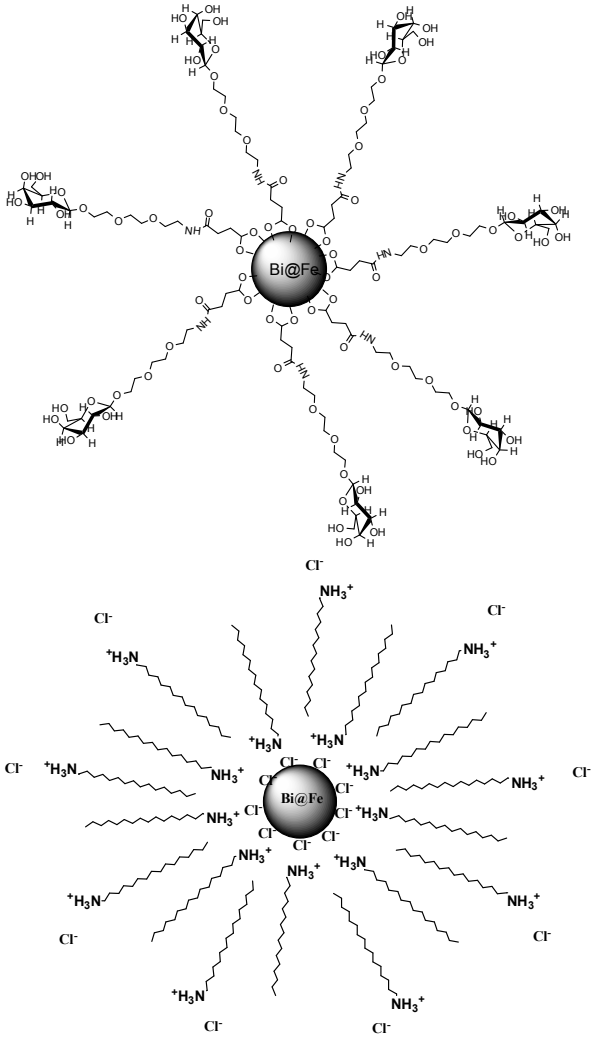

Figure 6: tentative schematic presentation of: top: LPEG1 coating on BiFe150. bottom: HDA.HCl double layer at the surface of BiFe14.

Faraday Discussions Accepted Manuscript

Unfortunately, if amine coating could be displaced easily from BiFe150, BiFe14 NPs prepared in the presence of HDA and its hydrochloride salt could not be functionalized by carboxylic acids, even with the simple oleic acid, as evidenced by IR spectroscopy. The passivation of the Fe rich surface is tentatively attributed to the coordination of chloride ions from HDA.HCl. Indeed, anchoring of chloride ions has been evidenced for cobalt NPs when chloroammonium salts were used for their stabilization, [38] and halide ions are reported to decrease the catalytic activity of iron NPs due to strong grafting on their surface[39] and tune the structure of Fe nanoparticles, once again because of the strong interaction between Fe and these ions.[40] Furthermore, it is noteworthy that these NPs were slightly soluble into water after extensive washing with ethanol. We suggest that the ammonium chloride organizes into a double layer around the NPs thus exposing polar heads towards the solution as shown in Figure 6 (bottom). Still, the colloidal solutions obtained this way were only stable over a few minutes.

From these results it is apparent that different strategies towards surface modification must be envisaged depending on the surface state of the NPs. Especially, BiFe14 NPs displaying the most interesting size in view of biomedical application, a proper method for their efficient stabilization in aqueous solutions must be designed.

Spontaneous oxidation.

The nanoobjects described here above have been prepared under inert atmosphere and are prone to oxidation as soon as they are exposed to air given the high reactivity of iron, especially at the nanoscale. It is noteworthy that this oxidation is a desirable event in view of biomedical applications as it will lead to nanohybrids displaying a surface state comparable to that of the SPION presently developed as MRI contrast agents.

BiFe14 NPs displaying the most interesting size in view of biomedical applications, spontaneous oxidation of these NPs was thus investigated. After one day of air exposure, observation of the (110) lattice planes of *rhombohedral* Bi (Figure 7, top) is a clear indication that the Bi core remains unchanged. However, the iron shell around seems now fully oxidized as attested by the observed lattice planes spacing (circa 0.25nm). Due to the small size of the iron oxide grains, it is difficult to establish their structural phase, especially as the observed lattice spacing is shared by all major iron oxides. Also, given the spontaneous character of the oxidation, different kinds of oxides and/or hydroxides are likely to form simultaneously. It is noteworthy that Mossbauer spectra present a weak signal over noise ratio probably due to the high absorption of the bismuth core preventing any investigation of the iron oxide nature by this technique.

After longer exposure time, crystallinity of the Bi core is lost (Figure 7, bottom) and full oxidation of the NPs is obtained. It is important to note that oxidation of the Bi core is not a limitation for the application envisaged as the X-Ray absorption doesn't depend on the oxidation state of an element.

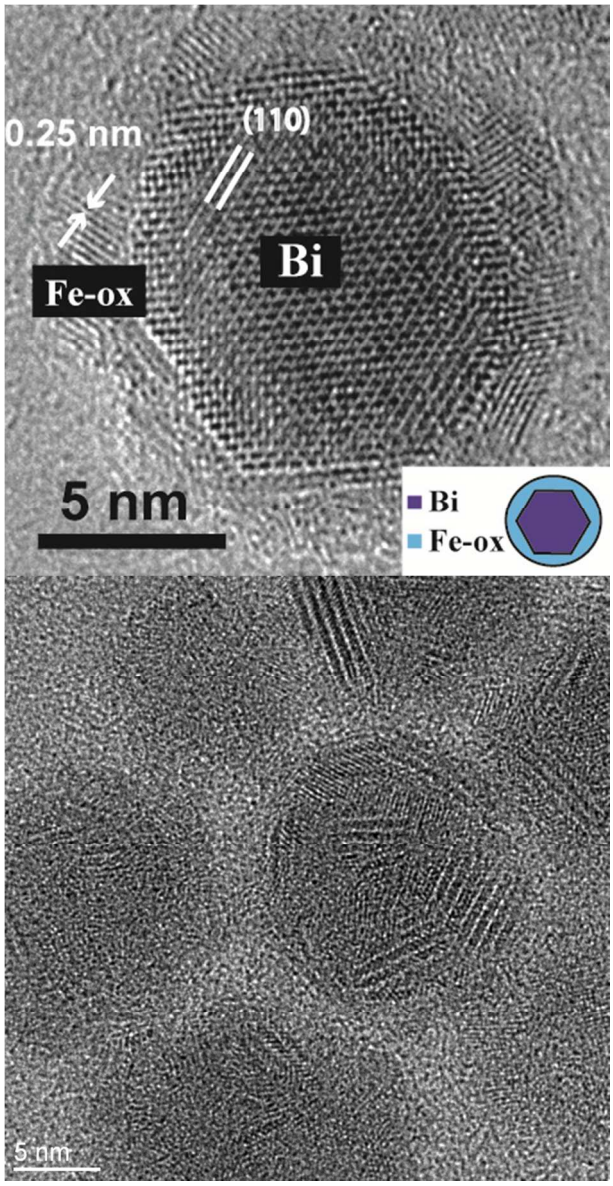

Figure 7: TEM images of BiFe14 after air exposure. top: after 2 days; bottom: after one year.

X-ray opacity and first MRI imaging results.

The possible activity of BiFe14 NPs as CT or MRI contrast agent was then investigated as the suspensions of NPs in water are magnetically responsive, evidencing the formation of a magnetic iron oxide. However, given the configuration of the external shell (similar to that of a hollow sphere), closure of stray fields should lead to a very weak overall magnetization. As a consequence of the small thickness of the shell (1 to 2.5 nm, with an inner diameter around 10nm), strong magnetic disorder and non collinear spin structures may occur, which could also lead to small magnetic moments carried by the nanoparticles. These features could lead to low activity as MRI contrast agent (to get high MRI sensitivity, the magnetic moment should be as high as possible) if any at all. However, at the nanoscale many surface defects are present and deviation from a perfect spherical symmetry is expected which may

Faraday Discussions Accepted Manuscript

This journal is © The Royal Society of Chemistry 2012

overcome the limitations discussed above. Preliminary tests were carried out to check if the local field produced by the oxide shell is strong enough to induce contrast. As the stability of the NPs in water is limited, homogeneity of the aqueous medium has been ascertained by gel formation with agar. Spin-spin relaxation time (T2) weighted spin echo MR Images of Bi-Fe nanohybrids are shown in Figure 8. Contrast enhancement varies as a function of the increase of the concentration of the nanomaterial, which suggests that it can be used as a contrast agent for MRI.

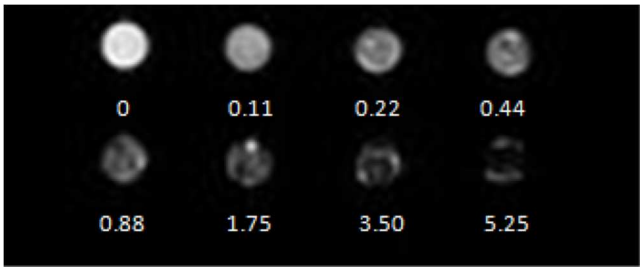

Figure 8: *T2*-weighted MRI of the Bi-Fe hybrid nanoparticles in agar gel at 3T as a function of Fe concentration (mmol.L^{-1}).

Compared to classical iodine based CT contrast agents, bismuth presents the advantage of a higher attenuation coefficient of X-Rays at 100keV due to the position of its K edge (90.8 keV). (X-ray absorption coefficient of bismuth is 5.74 cm^2 g^{-1} and that of iodine is 1.94 cm^2 g^{-1}, for comparison water absorption is only 0.171 cm 2 g $^{-1}$). Bismuth based NPs are thus perfectly adapted to color CT imaging, the newest advancement in CT imaging technology.[3] However, classical CT scanners operated at 100 kV, emit an X-ray spectrum from 30 keV to about 100 keV, with a maximum emitted intensity around 60keV. So the attenuation properties of the elements over the range 30-100 keV need to be considered as Iodine actually has better attenuation than bismuth at voltages below Bismuth's K-edge. We thus investigated the properties of BiFe14 in comparison to those of a commercial CT contrast agent: Omnipaque. This study, carried out on a CT scanner dedicated for small animals operated at 120 kV evidences an absorption coefficient twice that of Omnipaque, as observed for Bi_2O_3 NPs of similar size.[4] BiFe14 is thus a promising nano-platform for dual CT and MR imaging.

Conclusions and perspectives

In conclusion we have designed an efficient synthesis route to well crystallized core-shell Bi-Fe NPs that spontaneously oxidize into an intermediate Bi@FeOxide nanohybrid. As few data are available for Bi in the NP form,[41,5] the presence of Fe in the shell of the NPs providing a protecting barrier and isolating the Bi domain from the biological medium is important for safety reasons. These NPs give an enhanced contrast in CT imaging and significant contrast in MRI in vitro. They are thus promising cheaper alternatives to the FeAu dual contrast agents reported so far. Beyond their possible use in biomedical imaging, such nanohybrids open the perspective of a better tuning of the radiation dose in a precisely localized area of the body during X-Ray radiotherapy.[42] On-going work focuses on the optimization of their surface functionalization, and on the investigation of their magnetic behavior to correlate with their effect on T2 weighted MRI images.

Acknowledgements

This work has been supported by the ANR, the French National Research Agency (Mag@M project ANR-09-BLAN-0002-01). M. Branca thanks the Region Midi-Pyrénées and University Paul-Sabatier for a grant. We are also indebted to Dr. Puerto Morales for fruitful discussions, to Voxcan for CT measurements, Pr. Marc Verelst, Hélène Gros-Dagnac and M. Semyou-Ayele Osseni for their help in recording MRI images.

Notes and references

[a] CNRS, LCC (Laboratoire de Chimie de Coordination); 205, route de Narbonne, F-31077 Toulouse, France.
[b] Université de Toulouse, UPS, INPT; LCC; F-31077 Toulouse, France
[c] Department of Chemistry, National Tsing Hua University, 101, Sec. 2, Kuang-Fu Road, Hsinchu, Taiwan 30013 (Taiwan)
[d] CNRS, CEMES (Centre d'Elaboration des Matériaux et d'Etudes Structurales).
[e] LPCNO, INSA, 135 Avenue de Rangueil, 31077 Toulouse Cedex 4

[1] A. Jakhmola, N. Anton, and T. F. Vandamme, *Adv. Healthcare Mater.*, 2012, **1**, 413–431
[2] K. Ai, Y. Liu, J. Liu, Q. Yuan, Y. He, and L. Lu, *Adv. Mater.*, 2011, **23**, 4886.
[3] D. Pan, E. Roessl, J.-P. Schlomka, S. D. Caruthers, A. Senpan, M. J. Scott, J. S. Allen, H. Zhang, G. Hu, P. J. Gaffney, E. T. Choi, V. Rasche, S. A. Wickline, R. Proksa, and G. M. Lanza, *Angew. Chem. Int. Ed.*, 2010, **49**, 9635.
[4] H. Aviv, S. Bartling, I. Grinberg, and S. Margel, *J. Biomedical Mater. Res. Part B: Appl. Biomater.*, 2013, **101B**, 131.
[5] A. L. Brown, P. C. Naha, V. Benavides-Montes, H. I. Litt, A. M. Goforth, D. P. Cormode, *Chem. Mater.* **2014**, *26*, 2266.
[6] D. Danila, E. Johnson, P. Kee, *Nanomedicine: nanotechnology, biology and medicine* **2013**, *9(7),* 1067–1076.
[7] T. Zhou, B. Wu, D. Xing, *J. Mater. Chem.* **2012**, *22*, 470.
[8] P. Debbage, W. Jaschke, *Histochemistry And Cell Biology* **2008**, *130*, 845.
[9] M. Liong, J. Lu, M. Kovochich, T. Xia, S. G. Ruehm, A. E. Nel, F. Tamanoi, J. I. Zink, *ACS Nano* **2008**, *2*, 889–896.
[10] T. Courant, V. G. Roullin, C. Cadiou, M. Callewaert, M. C. Andry, C. Portefaix, C. Hoeffel, M. C. de Goltstein, M. Port, S. Laurent, L. V. Elst, R. Muller, M. Molinari, F. Chuburu, *Angew. Chem. Int. Ed.* **2012**, *51*, 9119
[11] D. Choi, A. Han, J. P. Park, J. K. Kim, J. H. Lee, T. H. Kim, S.-W. Kim, *Small* **2009**, *5*, 571
[12] X. Shao, H. Zhang, J. R. Rajian, D. L. Chamberland, P. S. Sherman, C. A. Quesada, A. E. Koch, N. A. Kotov, X. Wang, *ACS Nano* **2011**, *5*, 8967
[13] R. Ta, M. Suchy, J. H. K. Tam, A. X. Li, F. S. Martinez-Santiesteban, T. J. Scholl, R. H. E. Hudson, R. Bartha, S. H. Pasternak, *Contrast Media and Molecular Imaging* **2013**, *8*, 127.
[14] G. Pourroy, S. Begin-Colin, D. Felder-Flesch, French patent n° 1053139 (CNRS), France, **2010**.
[15] E. Pisani, N. Tsapis, B. Galaz, M. Santin, R. Berti, N. Taulier, E. Kurtisovski, O. Lucidarme, M. Ourevitch, B. T. Doan, J. C. Beloeil, B. Gillet, W. Urbach, S. L. Bridal, E. Fattal, *Adv. Func. Mater.* **2008**, *18*, 2963.
[16] F. Yang, Y. Li, Z. Chen, Y. Zhang, J. Wu, N. Gu, *Biomaterials* **2009**, *30*, 3882.
[17] D. Kim, M. K. Yu, T. S. Lee, J. J. Park, Y. Y. Jeong, and S. Jon, *Nanotechnology*, 2011, **22**, 155101

Faraday Discussions Accepted Manuscript

[18] A. Louie, *Chem. Rev.* **2010**, *110*, 3146.
[19] K. Nikolaou, M. Poon, M. Sirol, C. R. Becker, Z. A. Fayad, *Cardiology clinics* 2003, 21(4), 639-55.
[20] A. Hagit, B. Soenke, B. Johannes, M. Shlomo, *Biomacromolecules* **2014**, *11*, 1600.
[21] O. Rabin, J. M. Perez, J. Grimm, G. Wojtkiewicz, And R. Weissleder, *Nature Mater.*, 2006, **5**, 118
[22] M. Andrés-Vergés, M. d. P. Morales, S. Veintemillas-Verdaguer, F. J. Palomares, and C. J. Serna, *Chem. Mater.*, 2012, **24**, 319−324.
[23] M.Vehkamaki, T.Hatanpaa, M. Ritala, M.Leskela, *J. Mater. Chem.* 2004, **14**,3191–3197
[24] K.Soulantika, A.Maisonnat, M.-C.Fromen, M.-J.Casanove and B.Chaudret, *Angew. Chem. Int. Ed.*, 2003, **42**,1945
[25] I. G. Green and B. P. Roberts, *J. Chem. Soc., Perkin Trans.* 1986, **2**, 1597
[26] http://www.antellis.com/
[27] C.-H. Lai, C.-Y. Lin, H.-T. Wu, H.-S. Chan, Y.-J. Chuang, C.-T. Chen, C.-C. Lin, *Adv. Func. Mater.* 2010, **20**, 3948.
[28] D. Ciuculescu, C. Amiens, M. Respaud, A. Falqui, P. Lecante, R. E. Benfield and B. Chaudret, *Chem. Mater.* 2007, 19(19), 4624.
[29] N. Atamena, D. Ciuculescu, G. Alcaraz, A. Smekhova, F. Wilhelm, A. Rogalev, B. Chaudret, P. Lecante, R. E. Benfield, C. Amiens, *Chem. Commun.* 2010, **46**, 2453 – 2455.
[30] J. G. Mattei, F. Pelletier, D. Ciuculescu, P. Lecante, J. C. Dupin, N. Yaacoub, J. Allouche, J. M. Greneche, D. Gonbeau, C. Amiens, M.J. Casanove, *J. Phys. Chem. C* 2013, **117**, 1477.
[31] A. Meffre, S. Lachaize, C. Gatel, M. Respaud, B. Chaudret, *J. Mater. Chem.* 2011, **21**, 13464.
[32] X. Wang, R. D. Tilley, J. J. Watkins, *Langmuir* 2014, **30**, 1514.
[33] G. Huang, J. Diakur, Z. Xu, L. I. Wiebe, *Int. J. Pharm.,* 2008, **360**, 197.
[34] D.L. Morris, *Science*, 1948, **107**, 254
[35] K. Rahme, L. Chen, R. G. Hobbs, M. A. Morris, C. O'Driscoll, J. D. Holmes, *RSC Advances* 2013, **3**, 6085.
[36] A. G. Kanaras, F. S. Kamounah, K. Schaumburg, C. J. Kiely, M. Brust, *Chem. Commun.* 2002, 2294.
[37] E. E. Foos, A. W. Snow, M. E. Twigg, M. G. Ancona, *Chem. Mater.* 2002, **14**, 2401.
[38] H. Modrow, S. Bucher, J. Hormes, R. Brinkmann, H. Bönnemann, *J. Phys. Chem. B* 2003, **107**, 3684.
[39] K. Moore, B. Forsberg, D. R. Baer, W. A. Arnold, R. L. Penn, *J. Environmental Eng.* 2011, **137(10)**, 889-896.
[40] S. Zhang, G. Jiang, G. T. Filsinger, L. Wu, H. Zhu, J. Lee, Z. Wu, S. Sun, *Nanoscale* 2014, **6**, 4852.
[41] Y. Luo, C. Wang, Y. Qiao, M. Hossain, L. Ma, and M. Su, *J Mater Sci: Mater Med*, 2012, **23**, 2563–2573
[42] J. Zheng, G. Perkins, A. Kirilova, C. Allen, D. A. Jaffray, *Invest. Radiol.* 2006, **41**, 339.

Faraday Discussions Accepted Manuscript

 This journal is © The Royal Society of Chemistry 2012